Optics Letters

Microresonator-based high-resolution gas spectroscopy

Mengjie Yu,[1,2,*] Yoshitomo Okawachi,[1] Austin G. Griffith,[3] Michal Lipson,[4] and Alexander L. Gaeta[1]

[1]Department of Applied Physics and Applied Mathematics, Columbia University, New York, New York 10027, USA
[2]School of Electrical and Computer Engineering, Cornell University, Ithaca, New York 14853, USA
[3]School of Applied and Engineering Physics, Cornell University, Ithaca, New York 14853, USA
[4]Department of Electrical Engineering, Columbia University, New York, New York 10027, USA
*Corresponding author: my2473@columbia.edu

Received 14 July 2017; revised 29 September 2017; accepted 2 October 2017; posted 3 October 2017 (Doc. ID 302293); published 25 October 2017

We report the first demonstration of a microresonator-based tunable mode-locked frequency comb source. We achieve a mode-hop-free tuning range of 16 GHz by simultaneously tuning both the pump laser and the cavity resonance while keeping the system in a multi-soliton mode-locked state. The optical spectrum spans 2520–4125 cm^{-1} (2.425–3.970 μm) pumping at 3508 cm^{-1} (2.850 μm) in a silicon microresonator with a comb line spacing of 4.23 cm^{-1} (127 GHz). Our scanning technique can be used to increase the effective resolution of the microresonator-based comb spectroscopy. As a proof-of-principle demonstration, we record the absorption spectrum of the rovibrational transitions of the υ_3 and $\upsilon_2 + (\upsilon_4 + \upsilon_5)^0_+$ bands of acetylene. We measure absorption features as narrow as 0.21 cm^{-1} (6.4 GHz) full width at half-maximum at a frequency sampling step of 80 MHz.

OCIS codes: (300.6340) Spectroscopy, infrared; (190.4975) Parametric processes; (190.4390) Nonlinear optics, integrated optics.

https://doi.org/10.1364/OL.42.004442

Mid-infrared (mid-IR) frequency combs [1] can enable broadband gas-phase spectroscopy [2,3] with unprecedented measurement capabilities and new applications in medical diagnostics, astrochemistry, atmospheric monitoring, remote sensing, and industrial process control. An optical frequency comb (OFC) [4,5] is a broad optical spectrum consisting of evenly spaced, spectrally narrow lines. The frequency of each comb line can be written as $f_m = f_{ceo} + mf_r$, where f_{ceo} is the carrier-envelope offset frequency and f_r is the repetition frequency. Compared to tunable lasers, such broadband combs enable an accurate measurement of a large number of molecular absorption lines and species simultaneously in a complex environment [6]. The most widely used OFC is generated by a mode-locked femtosecond laser [4,7] and has been previously utilized for high-resolution spectroscopy [8,9]. Recently, there has been interest in the development of OFC sources in the mid-IR spectral region, where the molecules in the gas phase have strong fundamental vibrational transitions. However, extension of OFCs into the mid-IR has proven to be challenging. Nonlinear optical processes, such as difference frequency generation [10–13] and optical parametric oscillation [14–17], are often used to convert an OFC from the near-infrared (near-IR) to the mid-IR with additional system complexities. Recently, there has been significant progress and development of mode-locked lasers in the mid-IR [18,19]. In order to resolve narrow absorption features, spectrometers with high instrumental resolution are often required to resolve individual comb lines of a low-repetition-rate OFC. Comb-resolved molecular spectroscopy has been achieved using mode-locked lasers in dual-comb systems [20–23], high-resolution Fourier transform spectrometers (FTIR) [24], virtually imaged phase array (VIPA)-based spectrographs [9], Vernier spectroscopy [25–27], and fiber comb spectrometers [28]. Tuning the frequencies of the OFC and interleaving the spectra has been first demonstrated to further improve the spectral resolution [29] and then applied to Doppler-free Fourier transform spectroscopy [30]. The possibility of surpassing the resolution of FTIR and the VIPA technique has been demonstrated by scanning the repetition rate of the OFC [9,24,31]. In the mid-IR, where laser sources and high-quality photodetectors (or arrays) remain in development, significant challenges exist for developing newer mid-IR OFC-based spectrometers with higher sensitivity and higher resolution in more compact systems.

Recently, mid-IR OFCs using quantum cascade lasers (QCL) [32,33] and microresonators [34] have shown great promise as a new generation of highly compact spectrometers. Over the past decade, microresonator-based OFCs [34–47] have attracted tremendous interest since the platform enables highly compact devices and powerful dispersion engineering, which allows for broad optical bandwidths with moderate pump consumption [48]. Several demonstrations of direct-comb spectroscopy have been reported in the near-IR in silica [46], silicon nitride [45,49], and fluoride microresonators [37], and have been recently achieved in the mid-IR region using silicon microresonators [44]. However, OFCs in such miniature devices inherently have large repetition rates, typically from 10 to 1000 GHz, which precludes their use for high-spectral-resolution molecular spectroscopy.

Here we report the first demonstration of a microresonator-based scanning OFC spectrometer suitable for gas-phase spectroscopy. We demonstrate mode-hop-free tuning of the frequency of a mode-locked mid-IR frequency comb in a silicon microresonator over 0.53 cm^{-1} (16 GHz) via simultaneous tuning of temperature and pump laser frequency. The mode-locked comb spans 2520–4.25 cm^{-1} (2.425–3.970 μm) with a comb line spacing of 4.23 cm^{-1} (127 GHz). The absorption spectrum of acetylene in the gas phase is measured in the υ_3 and $\upsilon_2 + (\upsilon_4 + \upsilon_5)^0_+$ bands at a frequency sampling step of 80 MHz, despite using a low-resolution FTIR (15 GHz). This technique overcomes the resolution limitation induced by the ultra-small physical size of the integrated device and the instrumental line shape of the FTIR.

Our approach is shown schematically in Fig. 1(a). In a microresonator, the pump line is one mode of the OFC and has a fixed phase relationship with the rest of the generated comb lines. By joint frequency tuning of both the pump laser and its corresponding cavity resonance by one comb line spacing, the OFC can be scanned to cover any spectral point within the comb bandwidth without any gaps. In our case, the pump laser frequency is tuned via piezo control, and the cavity resonance is controlled via the thermo-optic effect [35,36,40–42]. The setup is shown in Fig. 1(b). A high-Q silicon microresonator with a 100-μm radius is dispersion engineered to have anomalous group-velocity dispersion beyond 3 μm for the fundamental transverse electric (TE) mode, similar to Yu, *et al.* [43]. The microresonator is pumped by a free-running continuous-wave (CW) optical parametric oscillator (OPO) at 3508 cm^{-1} (2.850 μm) (Argos Model 2400, <100 – kHz linewidth at an integration time of 30 ms). The free carriers (FC) generated from three-photon absorption (3PA) are extracted with an integrated p-i-n junction and used to monitor the intracavity dynamics [43]. A thermoelectric cooler (TEC) is used to control the temperature of the silicon device with an estimated thermal response time of <0.1 s. The output spectrum is measured using a commercial FTIR. As the CW pump laser is swept across the effective zero pump-cavity detuning, soliton mode locking is achieved, as indicated by observation of the soliton steps [50], which results in an OFC with narrow lines and low noise. In our experiment, a mode-locked mid-IR OFC is generated at a pump power of 45 mW, and the spectrum consists of 378 comb lines with a line spacing $f_r = 4.23$ cm^{-1}

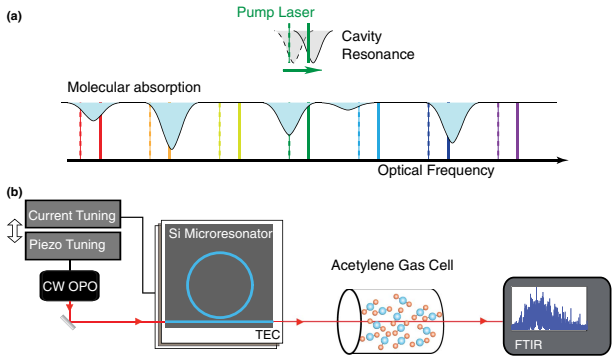

Fig. 1. (a) Scheme for scanning comb spectroscopy. (b) Experimental setup for microresonator-based scanning comb spectroscopy. CW OPO, continuous-wave optical parametric oscillator; FTIR, Fourier transform infrared spectrometer.

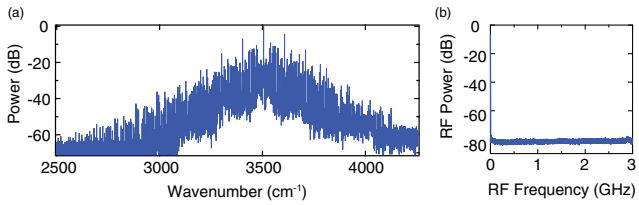

Fig. 2. (a) Optical spectrum of a mode-locked mid-IR frequency comb in a silicon microresonator. The full spectrum is collected using multiple band-pass filters before the FTIR. The modulated spectrum is indicative of a multiple-soliton state. (b) The radio-frequency spectrum of the extracted free-carrier current indicates generation of a low-noise frequency comb.

and spanning 2520–4125 cm^{-1}, as shown in Fig. 2. The DC component of the 3PA-induced-FC current is used to monitor the intracavity power and is especially sensitive to the soliton peak power and soliton numbers [43]. At the transition to mode locking, we observed a FC current jump from 0.8 to 1.2 mA, indicative of soliton formation. We then simultaneously manually tune both the pump frequency and the TEC current, which tunes the cavity resonance. During the tuning process, the DC component of the FC current is kept at 1.245 mA ± 0.001 mA in order to maintain the mode-locked state with the same soliton number and peak power. In our case, a multiple-soliton state is generated, which results in the variation of the power of the comb lines. The mode-hop-free tuning range of the frequency of the OFC is 0.53 cm^{-1}, which is 12.5% of f_r. It corresponds to a 100-mA change in the TEC current, which is a temperature change of about 25°C. Ideally, a tuning range of one free spectral range (FSR) will enable continuous coverage over the entire spectral range. Currently, our tuning range is limited by the pump power variations over the larger bandwidth.

We apply the scanning comb for an absorption measurement of the υ_3 and $\upsilon_2 + (\upsilon_4 + \upsilon_5)^0_+$ bands of acetylene in the gas phase. The output is recorded with an FTIR after a 2-cm-long single-pass cell, which is filled with 40 Torr of acetylene and 415 Torr of nitrogen. Using this method, scanning OFC spectroscopy can break the resolution limitation of the microresonator-based comb line spacing. The instrumental line shape of the FTIR is negligible due to a large comb line spacing. In our case, the FTIR is operated with a low resolution of 15 GHz, which enables fast acquisition. By monitoring the beat note between the pump laser and a femtosecond laser (Oria IR OPO), the pump frequency is tuned at 80-MHz steps. Figure 3(a) shows the recorded FTIR spectra. A band-pass filter with a center frequency of 3.77 cm^{-1} (3.250 μm) and a bandwidth of 470 cm^{-1} (0.5 μm) is used before the FTIR. The spectra of four selected comb lines are shown in Fig. 3(b). The measurement time of each spectrum is approximately 1 s, and the total measurement time is roughly 3 min. The frequency accuracy of the measurement is limited by the long-term stability of the pump laser, which is estimated to be <2 MHz over 1 s and <10 MHz over 3 min. Since the comb spacing is dependent on the chip temperature, the frequency shift of the pump mode is slightly different from that of the rest of the comb lines. Assuming the pump frequency $f_p = f_{ceo} + mf_r$, the index change as the pump is tuned by δf_p is $\delta n = -\frac{m*c}{L(f_p)^2} * \delta f_p$, where c and L are the speed

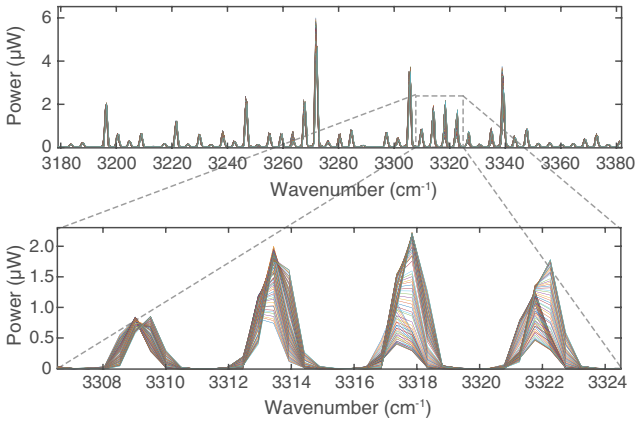

Fig. 3. FTIR spectra of acetylene absorption measurement. The OFC spectra is recorded at each 80 MHz of the pump shift with a low resolution of 15 GHz in the acetylene fingerprinting region (zoom-in: from 3185 to 3.78 cm^{-1}). The variation of the comb line power is largely attributed to the multiple soliton generation within the microresonator. The total measurement time is about 3 min. Bottom: the zoom-in plot shows the 2nd, 3rd, and 4th comb lines that overlap with the absorption features of the R(13), R(15), and R(17) lines of the $\upsilon_2 + (\upsilon_4 + \upsilon_5)^0_+$ band, respectively.

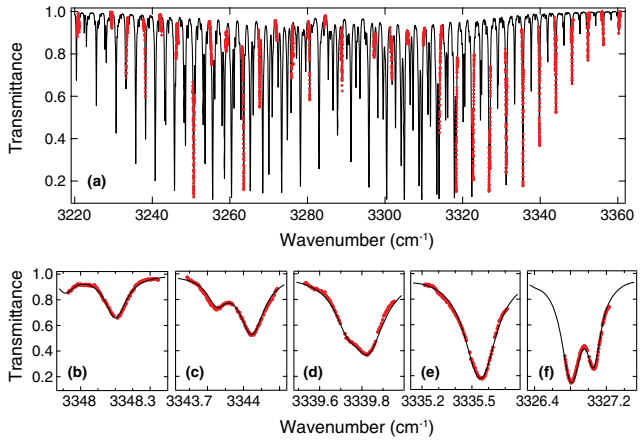

Fig. 4. (a) Measured transmittance spectrum (red circles) of the υ_3 and $\upsilon_2 + (\upsilon_4 + \upsilon_5)^0_+$ bands of acetylene is shown and compared to the computed transmittance profile (solid black line) using the HITRAN database. The transmittance is calculated as the ratio of the spectral powers with and without the gas cell. Transmittance (zoom-in) of five measured absorption features that correspond to (b) the R(23) line of the υ_3 band, (c) the R(27) line of the $\upsilon_2 + (\upsilon_4 + \upsilon_5)^0_+$ band (left) and the R(21) line of the υ_3 band (right), (d) the R(25) line of the $\upsilon_2 + (\upsilon_4 + \upsilon_5)^0_+$ band (left) and the R(19) line of the υ_3 band (right), (e) the R(17) line of the υ_3 band and the R(23) line of the $\upsilon_2 + (\upsilon_4 + \upsilon_5)^0_+$ band, (f) the R(13) line of the υ_3 band (left) and the R(19) line of the $\upsilon_2 + (\upsilon_4 + \upsilon_5)^0_+$ band (right).

of light in a vacuum and the cavity length, respectively. The change in the repetition rate can be expressed as $\delta f_r = -\frac{L(f_r)^2}{c} * \delta n = m\frac{f_r 2}{f_p} * \delta f_p$; thus, $\delta f_r = \delta f_p / m$. For the comb line $(n = N)$, $\delta f_{n=N} = (1 + \frac{N}{m})\delta f_p$, where the pump mode corresponds to $n = 0$ and the higher-frequency comb mode has $n > 0$. In our case, $m = 825$ and f_r changes from 127.23 to 127.25 GHz over the 16-GHz tuning range of the pump. Each comb line undergoes a different frequency shift, which equals to the product of its scaling factor and the pump shift. It must be taken into account for the frequency calibration through the scanning process. Figure 4 shows the calculated transmittance of acetylene in the υ_3 and $\upsilon_2 + (\upsilon_4 + \upsilon_5)^0_+$ bands. Figure 4(b) shows that our transmittance measurement successfully captures different absorption line shapes. The transmittance plot is compared to the computed transmittance profile using the HITRAN database with Lorentzian line shapes based on the condition of the gas cell. Figure 5(a) plots the absorption of the P(6) line of the $\upsilon_2 + (\upsilon_4 + \upsilon_5)^0_+$ band fitted with a Lorentzian profile. The full width at half-maximum (FWHM) linewidth is measured to be 0.213 cm^{-1} (6.4 GHz) centered at 3267.65 cm^{-1}. The fit residuals are shown in Fig. 5(b) and have a standard deviation of 4×10^{-3}. The signal-to-noise ratio (SNR) of the comb line is 23 dB measured by the FTIR, which limits the sensitivity of the measurement. The extracted line intensity is 6.87×10^{-20} cm/molecule. From the HITRAN data, the line intensity is 6.61×10^{-20} cm/molecule and the FWHM is 0.197 cm^{-1} (5.9 GHz) based on the self-broadening and nitrogen-broadening effect. Therefore, the deviation of the line intensity is 4% and that of the FWHM is 8%. The deviations can be attributed to the beat-note jitter between the CW pump laser and the femtosecond laser system (both free running) at each sampling point. Stabilization of both the pump laser and the reference laser would improve the precision of the sampling step. The frequency accuracy could be further improved through use of a stabilized OFC [38,39,47], for example, by self-referencing [47] or by locking to an atomic transition [38,39]. The SNR of the system could be further improved by averaging over multiple optical spectra, using the FTIR at a higher sensitivity mode and reduction of the pump power noise. As a proof-of-principle demonstration, the scanning technique allows for finer frequency measurements as compared to the typical microresonator-based comb line spacing.

In summary, we demonstrate a promising approach for a high-spectral-resolution spectroscopy using a scanning microresonator-based OFC with a comb line spacing of over 100 GHz. Rapid thermal tuning of the cavity resonance via

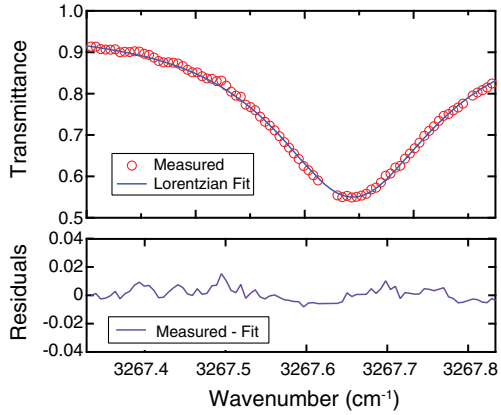

Fig. 5. Lorentzian profile (blue) fits the experimental measurement (red dots) of the P(6) line of the $\upsilon_2 + (\upsilon_4 + \upsilon_5)^0_+$ band. A FWHM of 0.21 cm^{-1} is measured centered at 3267.65 cm^{-1}. The standard deviation of the residuals (purple) is 4×10^{-3}.

an integrated heater (sub-millisecond level) [42] with a fully automatic scanning procedure would significantly improve the scanning rate. Integrating the heaters on such silicon microresonators with p-i-n structures could be challenging and has not yet been demonstrated. A flatter pump power would allow for a complete scan over one FSR to access the entire optical spectral range. A silicon microresonator with a larger radius will benefit from the current scanning range. In the mid-IR, commercial QCLs have shown a broadband tuning flexibility over 60 cm^{-1} (1.8 THz) and the potential to pump the microresonators. Recently, there has been progress on integration of QCLs on a silicon platform [51]. We believe that with continued development of QCLs, our technique would provide a compact spectrometer in the mid-IR with high sensitivity and high resolution for on-chip gas-phase spectroscopy.

Funding. Defense Advanced Research Projects Agency (DARPA) (W31P4Q-15-1-0015); Air Force Office of Scientific Research (AFOSR) (FA9550-15-1-0303); National Science Foundation (NSF) (ECS-0335765).

Acknowledgment. This work was performed in part at the Cornell Nano-Scale Facility, a member of the National Nanotechnology Infrastructure Network, which is supported by the NSF.

REFERENCES

1. A. Schliesser, N. Picqué, and T. W. Hänsch, Nat. Photonics **6**, 440 (2012).
2. M. Vainio and L. Halonen, Phys. Chem. Chem. Phys. **18**, 4266 (2016).
3. K. C. Cossel, E. M. Waxman, I. A. Finneran, G. A. Blake, J. Ye, and N. R. Newbury, J. Opt. Soc. Am. B **34**, 104 (2017).
4. T. Udem, R. Holzwarth, and T. W. Hänsch, Nature **416**, 233 (2002).
5. S. T. Cundiff and J. Ye, Rev. Mod. Phys. **75**, 325 (2003).
6. B. Spaun, P. B. Changala, D. Patterson, B. J. Bjork, O. H. Heckl, J. M. Doyle, and J. Ye, Nature **533**, 517 (2016).
7. D. J. Jones, S. A. Diddams, J. K. Ranka, A. Stentz, R. S. Windeler, J. L. Hall, and S. T. Cundiff, Science **288**, 635 (2000).
8. A. Marian, M. C. Stowe, J. R. Lawall, D. Felinto, and J. Ye, Science **306**, 2063 (2004).
9. S. A. Diddams, L. Hollberg, and V. Mbele, Nature **445**, 627 (2007).
10. F. C. Cruz, D. L. Maser, T. Johnson, G. Ycas, A. Klose, F. R. Giorgetta, I. Coddington, and S. A. Diddams, Opt. Express **23**, 26814 (2015).
11. I. Pupeza, D. Sánchez, J. Zhang, N. Lilienfein, M. Seidel, N. Karpowicz, T. Paasch-Colberg, I. Znakovskaya, M. Pescher, W. Schweinberger, V. Pervak, E. Fill, O. Pronin, Z. Wei, F. Krausz, A. Apolonski, and J. Biegert, Nat. Photonics **9**, 721 (2015).
12. C. R. Phillips, J. Jiang, C. Mohr, A. C. Lin, C. Langrock, M. Snure, D. Bliss, M. Zhu, I. Hartl, J. S. Harris, M. E. Fermann, and M. M. Fejer, Opt. Lett. **37**, 2928 (2012).
13. A. Gambetta, N. Coluccelli, M. Cassinerio, D. Gatti, P. Laporta, G. Galzerano, and M. Marangoni, Opt. Lett. **38**, 1155 (2013).
14. F. Adler, K. C. Cossel, M. J. Thorpe, I. Hartl, M. E. Fermann, and J. Ye, Opt. Lett. **34**, 1330 (2009).
15. L. Maidment, P. G. Schunemann, and D. T. Reid, Opt. Lett. **41**, 4261 (2016).
16. V. O. Smolski, H. Yang, S. D. Gorelov, P. G. Schunemann, and K. L. Vodopyanov, Opt. Lett. **41**, 1388 (2016).
17. M. Vainio and J. Karhu, Opt. Express **25**, 4190 (2017).
18. S. Antipov, D. D. Hudson, A. Fuerbach, and S. D. Jackson, Optica **3**, 1373 (2016).
19. S. Duval, M. Bernier, V. Fortin, J. Genest, M. Piché, and R. Vallée, Optica **2**, 623 (2015).
20. E. Baumann, F. R. Giorgetta, W. C. Swann, A. M. Zolot, I. Coddington, and N. R. Newbury, Phys. Rev. A **84**, 062513 (2011).
21. G. Millot, S. Pitois, M. Yan, T. Hovhannisyan, A. Bendahmane, T. W. Hänsch, and N. Picqué, Nat. Photonics **10**, 27 (2016).
22. S. Okubo, K. Iwakuni, H. Inaba, K. Hosaka, A. Onae, H. Sasada, and F.-L. Hong, Appl. Phys. Express **8**, 082402 (2015).
23. M. Yan, P.-L. Luo, K. Iwakuni, G. Millot, T. W. Hänsch, and N. Picqué, Light: Sci. Appl. **6**, e17076 (2017).
24. P. Maslowski, K. F. Lee, A. C. Johansson, A. Khodabakhsh, G. Kowzan, L. Rutkowski, A. A. Mills, C. Mohr, J. Jiang, M. E. Fermann, and A. Foltynowicz, Phys. Rev. A **93**, 021802 (2016).
25. C. Gohle, B. Stein, A. Schliesser, T. Udem, and T. W. Hänsch, Phys. Rev. Lett. **99**, 263902 (2007).
26. M. Siciliani de Cumis, R. Eramo, N. Coluccelli, M. Cassinerio, G. Galzerano, P. Laporta, P. De Natale, and P. Cancio Pastor, Phys. Rev. A **91**, 012505 (2015).
27. A. Gambetta, M. Cassinerio, D. Gatti, P. Laporta, and G. Galzerano, Sci. Rep. **6**, 35541 (2016).
28. N. Coluccelli, M. Cassinerio, B. Redding, H. Cao, P. Laporta, and G. Galzerano, Nat. Commun. **7**, 12995 (2016).
29. P. Jacquet, J. Mandon, B. Bernhardt, R. Holzwarth, G. Guelachvili, T. W. Hänsch, and N. Picqué, in *Advances in Imaging* (Optical Society of America, 2009), paper FMB2.
30. S. A. Meek, A. Hipke, G. Guelachvili, T. W. Hänsch, and N. Picqué, "Doppler-free Fourier transform spectroscopy," arXiv:1706.02974.
31. L. Rutkowski, P. Masłowski, A. C. Johansson, A. Khodabakhsh, and A. Foltynowicz, J. Quant. Spectrosc. Radiat. Transfer **204**, 63 (2018).
32. A. Hugi, G. Villares, S. Blaser, H. C. Liu, and J. Faist, Nature **492**, 229 (2012).
33. G. Villares, A. Hugi, S. Blaser, and J. Faist, Nat. Commun. **5**, 6192 (2014).
34. M. Yu, Y. Okawachi, A. G. Griffith, N. Picqué, M. Lipson, and A. L. Gaeta, "Silicon-chip-based mid-infrared dual-comb spectroscopy," arXiv:1610.01121.
35. P. Del'Haye, T. Herr, E. Gavartin, M. L. Gorodetsky, R. Holzwarth, and T. J. Kippenberg, Phys. Rev. Lett. **107**, 063901 (2011).
36. Y. Okawachi, K. Saha, J. S. Levy, Y. H. Wen, M. Lipson, and A. L. Gaeta, Opt. Lett. **36**, 3398 (2011).
37. C. Y. Wang, T. Herr, P. Del'Haye, A. Schliesser, J. Hofer, R. Holzwarth, T. W. Hänsch, N. Picqué, and T. J. Kippenberg, Nat. Commun. **4**, 1345 (2013).
38. A. A. Savchenkov, D. Eliyahu, W. Liang, V. S. Ilchenko, J. Byrd, A. B. Matsko, D. Seidel, and L. Maleki, Opt. Lett. **38**, 2636 (2013).
39. S. B. Papp, K. Beha, P. Del'Haye, F. Quinlan, H. Lee, K. J. Vahala, and S. A. Diddams, Optica **1**, 10 (2014).
40. H. Jung, K. Y. Fong, C. Xiong, and H. X. Tang, Opt. Lett. **39**, 84 (2014).
41. X. Xue, Y. Xuan, C. Wang, P.-H. Wang, Y. Liu, B. Niu, D. E. Leaird, M. Qi, and A. M. Weiner, Opt. Express **24**, 687 (2016).
42. C. Joshi, J. K. Jang, K. Luke, X. Ji, S. A. Miller, A. Klenner, Y. Okawachi, M. Lipson, and A. L. Gaeta, Opt. Lett. **41**, 2565 (2016).
43. M. Yu, Y. Okawachi, A. G. Griffith, M. Lipson, and A. L. Gaeta, Optica **3**, 854 (2016).
44. A. G. Griffith, R. K. W. Lau, J. Cardenas, Y. Okawachi, A. Mohanty, R. Fain, Y. H. D. Lee, M. Yu, C. T. Phare, C. B. Poitras, A. L. Gaeta, and M. Lipson, Nat. Commun. **6**, 6299 (2015).
45. A. Dutt, C. Joshi, X. Ji, J. Cardenas, Y. Okawachi, K. Luke, A. L. Gaeta, and M. Lipson, "On-chip dual comb source for spectroscopy," arXiv:1611.07673.
46. M.-G. Suh, Q.-F. Yang, K. Y. Yang, X. Yi, and K. J. Vahala, Science **354**, 600 (2016).
47. P. Del'Haye, A. Coillet, T. Fortier, K. Beha, D. C. Cole, K. Y. Yang, H. Lee, K. J. Vahala, S. B. Papp, and S. A. Diddams, Nat. Photonics **10**, 516 (2016).
48. Y. Okawachi, M. R. E. Lamont, K. Luke, D. O. Carvalho, M. Yu, M. Lipson, and A. L. Gaeta, Opt. Lett. **39**, 3535 (2014).
49. N. G. Pavlov, G. Lihachev, S. Koptyaev, E. Lucas, M. Karpov, N. M. Kondratiev, I. A. Bilenko, T. J. Kippenberg, and M. L. Gorodetsky, Opt. Lett. **42**, 514 (2017).
50. T. Herr, V. Brasch, J. D. Jost, C. Y. Wang, N. M. Kondratiev, M. L. Gorodetsky, and T. J. Kippenberg, Nat. Photonics **8**, 145 (2014).
51. A. Spott, J. Peters, M. L. Davenport, E. J. Stanton, C. D. Merritt, W. W. Bewley, I. Vurgaftman, C. S. Kim, J. R. Meyer, J. Kirch, L. J. Mawst, D. Botez, and J. E. Bowers, Optica **3**, 545 (2016).